Kinesin Superfamily Protein 3 (KIF3) Motor Transports Fodrin-associating Vesicles Important for Neurite Building

Sen Takeda, Hiroto Yamazaki, Dae-Hyun Seog, Yoshimitsu Kanai, Sumio Terada, and Nobutaka Hirokawa

Department of Cell Biology and Anatomy, University of Tokyo, Graduate School of Medicine, 7-3-1, Hongo, Bunkyo-ku, Tokyo 113-0033, Japan

Abstract. Kinesin superfamily proteins (KIFs) comprise several dozen molecular motor proteins. The KIF3 heterotrimer complex is one of the most abundantly and ubiquitously expressed KIFs in mammalian cells. To unveil the functions of KIF3, microinjection of function-blocking monovalent antibodies against KIF3 into cultured superior cervical ganglion (SCG) neurons was carried out. They significantly blocked fast axonal transport and brought about inhibition of neurite extension. A yeast two-hybrid binding assay revealed the association of fodrin with the KIF3 motor through KAP3. This was further confirmed by using vesicles collected from large bundles of axons (cauda equina), from which membranous vesicles could be prepared in pure preparations. Both immunoprecipitation and immunoelectron microscopy indicated the colocalization of fodrin and KIF3 on the same vesicles, the results reinforcing the evidence that the cargo of the KIF3 motor consists of fodrin-associating vesicles. In addition, pulse-labeling study implied partial comigration of both molecules as fast flow components. Taken together, the KIF3 motor is engaged in fast axonal transport that conveys membranous components important for neurite extension.

Key words: kinesin superfamily protein 3 • fodrin • microinjection • axonal transport • yeast two-hybrid

Introduction

The neuron is an example of a highly differentiated cell whose structure embodies its inherent manifold functions. The fine arborization of the dendrites and axons of neurons is adapted to the information processing taking place in the cell body. Due to the extreme specialization of the axon for transport, it is devoid of the machinery required for protein synthesis, which is an essential prerequisite for maintenance of the structures and functions of the axons and synapses. To deliver the required materials to the synapse, the neuron has a specialized machinery for axonal transport, where two major cytoskeletal structures (microfilaments and microtubules) serve as tracks. Microtubules (MTs)[1] are considered to play major roles in long-distance transport, whereas actin filaments are believed to be responsible for relatively short distance trafficking. During the past decade, subsequent to the discovery of kinesin (Brady, 1985; Vale et al., 1985) as a motor protein, several unique MT-dependent motor proteins have been identified and characterized in various living species. The kinesin superfamily proteins (KIFs; Aizawa et al., 1992; Hirokawa, 1996, 1998) are a collection of such motor proteins, most of which work as motors for anterograde transport along the MTs to their plus ends.

The KIF3 motor is one of the most abundantly and ubiquitously expressed KIFs, predominantly found in the nervous system. It is composed of a heterotrimeric complex formed with KIF3A (Aizawa et al., 1992; Kondo et al., 1994), either KIF3B (Yamazaki et al., 1995) or KIF3C (Muresan et al., 1998; Yang and Goldstein, 1998), and an associated protein, KAP3 (Yamazaki et al., 1995, 1996). This protein complex also has phylogenic diversity, blanketing a broad range of organisms from the sea urchin (kinesin II; Cole et al., 1993), *Chlamydomonas reinhardtii* (FLA10; Walther et al., 1994), *Caenorhabditis elegans* (Cekinesin II; Signor et al., 1999), *Drosophila melanogaster* (KLP68D; Pesavento et al., 1994), *Xenopus laevis* (Xklp3; Le Bot et al., 1998), and *Rana rugosa* (mKIF3A; Nakajima et al., 1997), to the green sunfish (*Lepomis cy-*

Address correspondence to Nobutaka Hirokawa, Department of Cell Biology and Anatomy, University of Tokyo, Graduate School of Medicine, 7-3-1, Hongo, Bunkyo-ku, Tokyo 113-0033, Japan. Tel.: +81-3-5841-3326. Fax:+81-3-5802-8646.

[1]*Abbreviations used in this paper:* aa, amino acids; CyDy, cytoplasmic dynein; KIF, kinesin superfamily protein; MT, microtubule; SCG, superior cervical ganglion.

anellus photoreceptor KIF3 antigen; Beech et al., 1996), implying its importance. The results of our previous study (Yamazaki et al., 1995) provided morphological evidence of the association of KIF3 with vesicles 90–160 nm in diameter that are biochemically isolated from the large bundles of axons (cauda equina) in the rat. Furthermore, several recent papers have reported the localization of KIF3 in greater detail, namely, that the KIF3 motor is installed within cilioflagellar structures, such as the connecting cilia of retinal rod cells (Muresan et al., 1997), embryonal sea urchin cilia (Morris and Scholey, 1997), and *Chlamydomonas* flagella (Kozminski et al., 1995; Cole et al., 1998; Rosenbaum et al., 1999). Surprisingly, the latest knockout studies on KIF3A (Marszalek et al., 1999; Takeda et al., 1999) and KIF3B (Nonaka et al., 1998) revealed the importance of KIF3 for left–right determination through ciliogenesis of nodal cells. Furthermore, it was demonstrated that the nodal cilia, in which KIF3A/B are localized, are rotating to generate unidirectional flow of extraembryonic fluid (nodal flow), which fundamentally controls left–right determination (Nonaka et al., 1998; Takeda et al., 1999).

Although the functions of the KIF3 family in nonneuronal systems have been intensively studied in various kinds of cells (Aizawa et al., 1992, Kondo et al., 1994; Yamazaki et al., 1995, 1996; Muresan et al., 1997; Cole et al., 1998; Le Bot et al., 1998; Nonaka et al., 1998; Tuma et al., 1998; Marszalek et al., 1999; Takeda et al., 1999), there remain large frontiers for us to reveal the function of KIF3 in neurons since it is abundantly expressed in the nervous system (Aizawa et al., 1992; Kondo et al., 1994; Pesavento et al., 1994; Yamazaki et al., 1995). Recent evidence suggested that *Drosophila* homologues of KIF3, i.e., KLP64D and KLP68D, are expressed in cholinergic neurons and are engaged in the axonal transport of choline acetyl transferase (Ray et al., 1999), although the functions of vertebrate KIF3 have not been elucidated yet. In the present study, we microinjected a monovalent Fab fragment of the anti-KIF3B antibody, which functionally hampers the motility of KIF3A/B heterodimers, into the cultured superior cervical ganglion (SCG) neurons to monitor the function of KIF3 motor in neuron. Furthermore, to investigate the results of microinjection experiments and to determine the way of cargo-binding of KIF3 motor, yeast two-hybrid binding assay was carried out. Subsequently, the physiological relevance of the obtained clones were examined by the combination of strategies, such as immunoprecipitation, immunoelectron microscopy, and pulse-labeling study.

Materials and Methods

Cell Culture of SCG Neurons

The culture of SCG neurons was carried out according to Takenaka et al. (1992), with slight modifications. In brief, C57BL mice aged 4–6 wk were killed by deep narcosis using diethyl ether. We cut open the neck region to reach the SCG, located just beneath the region where the common carotid artery branches into the external and internal carotid artery. The extirpated pairs of SCGs were briefly rinsed, cut into small pieces with a surgical blade, and bathed in HBSS. We incubated these small pieces in 1% trypsin (Sigma Chemical Co.) for 1 h, and then subjected them to 1% collagenase digestion (Worthington Biomedical Co.) for 3 h. During both enzymatic digestion procedures, the plastic tubes containing the tissue pieces were shaken in an air incubator heated at 37°C, to facilitate dissociation. Finally, we gently triturated the small SCG pieces after adding culture media for neutralizing the enzymes. The dissociated cells were plated on coverslips coated with collagen type IV (Sigma Chemical Co.) overlaid on poly-D-lysine, and grown in serum-free media to obtain unipolar neurons (Higgins et al., 1991).

Antibody Characterization and Fab Preparation

In the present work, we prepared Fab fragments from an affinity-purified anti-KIF3B antibody (Yamazaki et al., 1995), and from chromatographically purified normal mouse IgG (Zymed Labs) as a control. For obtaining the Fab fragments, we used the Fab preparation kit (Pierce Chemical Co.) according to the manufacturer's instructions. The resultant purified Fabs were concentrated to ~4 mg/ml by ultrafiltration (CENTRICON; Pharmacia Biotech), and dialyzed against potassium (K) glutamate injection buffer (50 mM potassium glutamate, 100 mM KCl, and 1 mM $MgCl_2$, pH 6.8) as described elsewhere (Funakoshi et al., 1996). The purity of Fab was confirmed by SDS gel electrophoresis. For the microinjection, we diluted the concentrated Fabs with K-glutamate buffer containing fluorescently labeled BSA to 3 mg/ml. Other antibodies used in this study were commercially available or developed by us: anti–αII-fodrin antibody (Biogenesis Ltd.); anti-KIF1A (Okada et al., 1995b); anti-KAP3 antibody (Yamazaki et al., 1996); anti-KIF5A antibody (Kanai, Y., Y. Okada, Y. Tanaka, A. Harada, S. Terada, and N. Hirokawa, manuscript in preparation); and anti-KIF5B antibody (Kanai, Y., Y. Okada, Y. Tanaka, A. Harada, S. Terada, and N. Hirokawa, manuscript in preparation).

Immunofluorescence Microscopy and Western Blotting of SCG

The immunofluorescence study of SCG cells was performed as described previously (Takeda et al., 1994) with minor changes (Muresan et al., 1998). The preparations were observed by BioRad confocal laser scanning microscopy. We also carried out Western blotting using the procedure previously described (Takeda et al., 1999).

Microinjection of Fab into SCG Cells

We microinjected the above mentioned anti-KIF3B Fab or normal mouse IgG Fab into the cultured SCG neurons at a concentration of ~3 mg/ml, as described previously (Brady et al., 1990; Takeda et al., 1994, 1995). As we reported previously (Yamazaki et al., 1995), this anti-KIF3B antibody specifically blocks the motility of KIF3A/B heterodimers in a concentration-dependent manner. For the identification of the injected cells, we coinjected fluorescein-labeled BSA (Takeda et al., 1994). For the vesicle traffic assay, the microinjections were carried out into SCG neurons with mature single axons displaying a relatively flat morphology and firmly attached to the substrate (~2 d after plating), for ease of observing the vesicle traffic by VEC–DIC microscopy. In this case, the concentration of antibody within the neurons is calculated to be 0.1–0.2 mg/ml, provided that the injected volume is 10^{-10} ml (Okabe and Hirokawa, 1988) and the volume of neurons is 4×10^{-9} ml (provided that the cell bodies of the neurons used in our experiment have a diameter of ~20 μm and height of ~10 μm, the axons being 2 μm in diameter and 600 μm in length). Since the Fab fragments have a molecular weight of about one-third that of native IgG, their molar concentration within the neuron should be at least 0.3–0.6 mg/ml, the value being higher than the minimal concentration required to completely block the motility of KIF3 in vitro. For the neurite extension inhibition assay, we selected neurons without neurites for microinjecting the antibodies (~12–20 h after plating), so that the concentration became much higher (at least twofold higher than that in the vesicle-blocking study) in this case.

Observation and Data Collection

An Olympus IX-70 microscope (Olympus Optics Co.) equipped with VEC–DIC/FL gadgetry was used for observing and recording the vesicle traffic within axons (Okada et al., 1995a). The entire microscope was installed inside a plastic chamber in which the temperature was controlled to ~37°C (Takenaka et al., 1992) using a thermostat. We repeated each pair of experiments seven times independently on different days. Each session consisted of 5–7 experimental runs, where microinjected neurons that were viable and appeared normal were chosen randomly for VEC–DIC observation. For the control experiment, we took records of 35 cells, whereas for the anti-KIF3 Fab series, 32 neurons were recorded. Each ob-

servation was videotaped for 5 min. Vesicular structures moving both centrifugally and centripetally were captured in the same video frames. Considering the demilune shape of an axonal cross-section, the volume of organelle traffic was calibrated by the cross-sectional area of the axon. Therefore, the ordinate in Fig. 5 indicates the number of vesicles passing through one square micrometer of the axon (~200–400 μm downstream from the cell body) per 5 min. For the neurite sprouting inhibition assay, the neurite lengths of cells identified under the fluorescence microscope were measured ~12 h after microinjection of Fabs. In brief, the cells grown on coverslips were fixed with 2% paraformaldehyde, mounted on glass slides, and photographed. Measurement of neurite length was performed on these photographs. We observed 60 cells injected with anti-KIF3B Fab and 50 injected with control IgG Fab. Each experimental session consisted of 5–6 independent experimental trials. We used *t* tests to compare the mean value of the vesicle in anti-KIF3B Fab-injected group with that of the control group. The level of significance was set at $P < 0.05$.

Construction of cDNA Libraries for Yeast Two-Hybrid Screening

Mouse total brain RNA was prepared from 5-d-old ICR pups using the Total RNA Separator Kit (Clontech), followed by isolation of mRNA from this preparation with the aid of the mRNA Separator Kit (Clontech). Then, cDNA libraries were prepared using the SuperScript choice system (GibcoBRL) with random hexamer primers. The cDNA library was ligated with EcoRI/NotI/SalI adaptors and inserted into the pBD42AD vector. We transformed ElectroMAX DH10B cells (GibcoBRL) with this construction and in turn obtained 6×10^6 independent clones. Finally, the plasmids were purified using the QUIAGEN Plasmid Kit.

Screening of KAP3-binding Proteins by Yeast Two-Hybrid Assay

A Matchmaker LexA two-hybrid system was used for the screening according to the instructions provided by the manufacturer (Clontech). In brief, a part of the KAP3 gene (amino acids [aa] 209–384, containing arm repeats 2–4) was fused to the DNA-BD region of the pLexA vector by the PCR method. Then the plasmid was cotransfected with the above mentioned library plasmids into the yeast strain EGY48 carrying the p8op-lacZ gene, grown on a SD/−His/−Trp/−Ura plate supplemented with glucose. Selection of positive clones was performed on a SD/−His/−Trp/−Ura/−Leu plate containing galactose/raffinose/X-gal/BU salts. Subsequent to these procedures, the bait plasmids were recovered from the positive clones to confirm whether the observed interaction was genuine, by retransformation into the yeast. We repeated these procedures several times and analyzed their sequences for which interaction was reproducibly ascertained.

β-Galactosidase Activity in Liquid Cultures of Yeast

The β-galactosidase activity in liquid cultures of yeast was assayed as described previously (Ausubel et al., 1997). In brief, mid-log phase yeast cells were collected and permeabilized with 0.1% sodium dodecyl sulphate (SDS) and chloroform. The chromogenic substrate o-nitrophenyl-β-D-galactoside was added in excess to this lysate, and after incubation at 30°C, the reaction was stopped by increasing the pH to 11, by the addition of 1 M Na_2CO_3. The OD at 420 nm, which corresponds to the absorbance by the reaction product, o-nitrophenol, was determined by spectrophotometry and normalized to the reaction time and the cell density.

Preparation and Immunoprecipitation of Vesicular Components from the Rat Cauda Equina

The preparation of cauda equina vesicles was carried out according to a previously reported method (Okada et al., 1995b), with slight modifications. In brief, two sets of cauda equina extirpated from dead female SD rats were put into 1 ml of IM-D buffer, supplemented with a protease inhibitor cocktail (Sigma Chemical Co.) and 1 mM ATP, and minced with a pair of ophthalmological scissors for 5 min. After 5-min incubation on ice, they were minced again for 5 min. Under this condition, KIF motor proteins became detached from the MTs, enabling us to isolate the vesicles harboring KIFs. In addition, contamination of axolemmal components could be avoided, as the samples were never homogenized. The resultant suspension was subjected to centrifugation at 10,000 rpm for 10 min at Kubota's benchtop centrifugator, to eliminate gross fragments of the axonal sheath. The obtained supernatant, rich in axonal vesicles, was used for further analysis.

For immunoprecipitation, protein A–Sepharose beads (Pharmacia Biotech) were coupled with either anti-KIF3B, KAP3, α-fodrin, or preimmune serum as described previously (Okada et al., 1995b). In brief, polyclonal antibodies against KAP3, KIF1A (1 mg each), and mAb against αII-fodrin (1 mg) were bound to 15 ml of fresh protein A–Sepharose 4B beads (Pharmacia Biotech) in TBS containing 1% Triton X-100 (TBST) for 2 h at 4°C before the immunoprecipitation. Uncoupled antibody was removed by washing the beads five times in TBST. The above mentioned vesicle fractions were incubated overnight with antibody-coupled Sepharose beads, and thoroughly washed three times with IM-D. Then the beads were incubated with IM-D containing 1% Triton X-100 for 1 h on ice, followed by washing with IM-D twice. Finally, the obtained beads were processed for SDS gel electrophoresis, transferred to a membrane, and prepared for Western blotting.

Negative Staining of the Cauda Equina Vesicles

The cauda equina vesicles prepared as above were subjected to immunoelectron microscopy and negative staining according to the method reported by Nishiye et al. (1988), with slight modifications (Takeda et al., 1994). After random observation and electron microscopic photography (JEOL 1200Ex), the frequency of the colocalization of gold-labeling for KIF3B and fodrin was determined as follows. We categorized the parameter into the following three sections: single-labeling with either anti-KIF3B antibody or anti–αII-fodrin antibody; double-labeling with both anti–αII-fodrin and anti-KIF3B antibodies; and control normal mouse IgG/preimmune serum. The labeling frequency was calculated by dividing the total number of vesicles with that of vesicles harboring colloidal gold. Then, the obtained values were calibrated with that of negative control. 38 pictures containing 454 vesicles were quantified for their labeling frequency. The background colloidal gold per cm^2 (colloidal gold signals that did not associate with vesicles) was also calculated, and it was subtracted from the frequency of labeling. About 54% of all vesicles were labeled with either anti-fodrin antibody or anti-KIF3B antibody.

Immunoelectron Microscopy of the Mouse Cauda Equina Vesicles

Immunoelectron microscopy of the biochemically purified cauda equina vesicles was carried out according to the method reported by De Camilli et al. (1983). In brief, a small aliquot (50 ml) of the cauda equina preparation (Okada et al., 1995b) was mixed with a solution of ~2% agarose in an Eppendorf tube at 37°C, followed by immediate placement on ice. Solidified agarose gel was carefully detached from the tube and cut into small pieces with a surgical blade. These agarose blocks containing the fixed cauda equina vesicles were further processed for immunoelectron microscopy as described previously (Takeda et al., 1994), with modifications in the incubation times. For the first antibody, the agarose blocks were incubated for 24 h at 4°C with gentle shaking. Since the colloidal gold-conjugated second antibody does not easily penetrate into the agarose meshwork, we incubated the agarose block for ~2 d at 4°C, rotating the reaction tube of agarose blocks. After postfixing with half Karnovsky solution and 1% OsO_4, the samples were stained overnight with 1% uranyl acetate, and then completely dehydrated. Finally, they were embedded in epoxy resin. Ultrathin sections of these blocks were cut and observed by JEOL 1200Ex.

Pulse–Chase of KIF3B by Metabolic-labeling in the Rat Optic Nerve

The velocities of motor proteins in vivo and the transport of fodrin were measured according to Elluru et al. (1995). In brief, 1 mCi/4ml of an [^{35}S]methionine and [^{35}S]cystein mixture (New England Nuclear Life Science Products) was injected into the vitreous of the SD rat eyeball (12-wk-old, male). The animals were killed 4, 6, and 8 h after injection for all the experiments, except those on KIF1A. For the KIF1A experiment, we collected samples 1.6, 2, and 3 h after injection. The optic tract was extirpated en bloc and was divided into proximal (5–10 mm from eyeball) and distal (10–15 mm idem) parts.

Next, all the segments were homogenized in 300 μl of axon lysis buffer (50 mM NaCl, 25 mM Tris, pH 8.1, 0.5% Triton X-100, 0.5% sodium

deoxycholate, 2 mM sodium orthovanadate, 50 mM NaF, 100 mM KPO_4, 25 mM sodium pyrophosphate, 80 mM β-glycerophosphate, 1 mM PMSF, 10 μg/ml pepstatin A, 2 μg/ml aprotinin, 4.5 mM EDTA, 1 mM benzamidine, and 10 μg/ml leupeptin), using a polytron microhomogenizer. The homogenate was then centrifuged at 15,000 rpm for 10 min at 4°C and the supernatant (S1) was collected (crude extract; this sample was also subjected to SDS-PAGE analysis).

The antibody-conjugated beads were added to S1, and the mixture was left to stand for 3–4 h at 4°C. After the reaction, the beads were washed five times with TBST. Finally, each sample was processed by conventional SDS-PAGE. The gels were dried, exposed to a fluorogram, and read using a digitized image analyzer (Fuji Bas).

Results

Characterization of Anti-KIF3B Antibody

As previously reported, our anti-KIF3B antibody revealed binding uniquely with the 85-kb polypeptide in SCG extracts (Fig. 1 D, lane 1), while preimmune sera did not (Fig. 1 D, lane 2). Immunofluorescence of cultured SCG neurons (Fig. 1 A) also revealed the localization of this protein, both in the cell body and the axons, the latter of which partly showed a punctate staining pattern (Fig. 1 C). With the previous ultrastructural finding that KIF3 is associated with vesicles isolated from cauda equina (Yamazaki et al., 1995), this staining pattern is considered to represent the association of KIF3 with axonal membranous components. As shown in our previous study (Yamazaki et al., 1995), this anti-KIF3B antibody blocks the in vitro motility of KIF3A/B heterodimers in a concentration-dependent manner.

Reduction of Fast Axonal Transport after Anti-KIF3B Fab Injection

To test the consequence of inhibiting KIF3 function, Fab fragments prepared from either anti-KIF3B antibody or normal mouse IgG (~3 mg/ml) were injected. To avoid possible cross-linking of vesicles to one another, resulting in a nonspecific traffic jam, Fab fragments were used.

About three hours after microinjection, we observed the SCG neurons emitting dim green fluorescence under the low-light level fluorescence microscope system equipped with the VEC–DIC system. Under the VEC–DIC, the ratio of the different categories of vesicles did not seem to have changed as a result of antibody injection (Fig. 2), but the number of vesicle passing through a certain point on the axon distant from the cell body (~200–400 mm) was significantly decreased (Fig. 2). Vesicle movements were quantified (Fig. 3 C), revealing that the microinjection process, per se, did not seem to have any deleterious effect on vesicle traffic, as injection of the control antibody gave almost the same results, as compared to uninjected samples (except for mitochondria, all groups show comparable vesicle traffic to the noninjected group). However, anti-KIF3B antibody injection dramatically diminished the total vesicle traffic along axons (Figs. 2 A and 3 B, control, 29.0 ± 0.3; anti-KIF3B Fab, 9.4 ± 0.1, mean ± SEM). In particular, the anterograde traffic (control, 13.7 ± 0.2; anti-KIF3B Fab, 3.8 ± 0.1; 27.5% of noninjected group) was more severely affected than that of retrogradely moving vesicles (control, 15.3 ± 0.2; anti-KIF3B Fab, 5.6 ± 0.2; 35.8% of noninjected control), the results reflecting the nature of KIF3 as an anterograde motor. Since mitochondria did not often move and were only infrequently observed in the SCG, it was difficult to judge whether mitochondrial traffic (control, 1.8 ± 0.1; anti-KIF3B Fab, 1.0 ± 0.1) was influenced or not. However, *t* test revealed no significant difference in mean values at the significance of $P < 0.05$, whereas other groups were significantly different at the level of $P < 0.001$. In addition, in COS cells or embryonic Reichert's membrane cells enriched in mitochondria, we could not observe any inhibitory effects of anti-

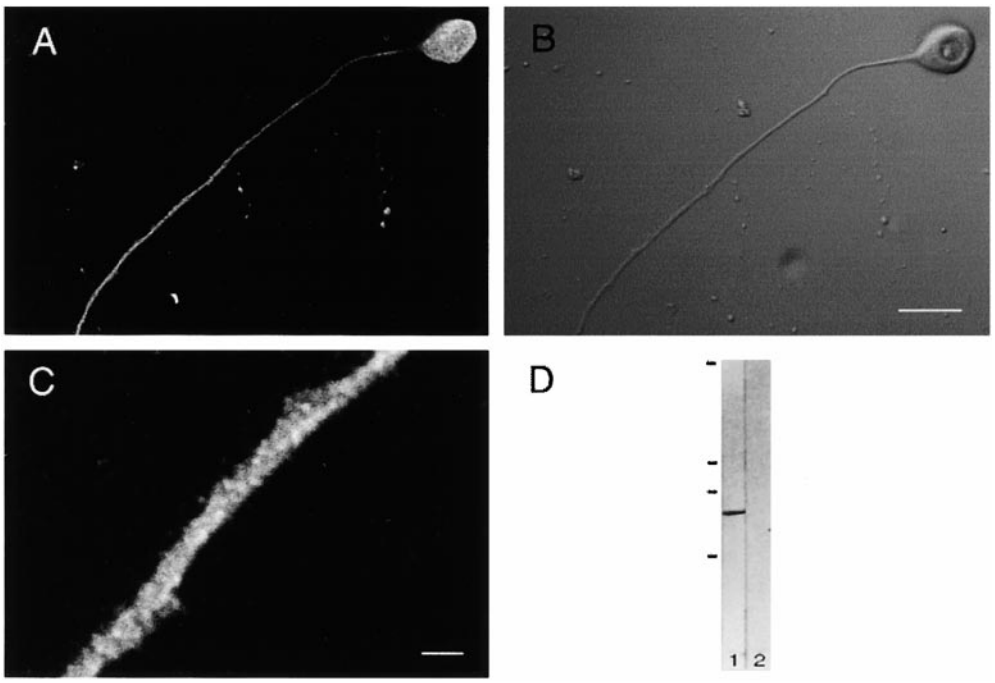

Figure 1. Characterization of anti-KIF3B antibody. A, Fluorescence immunocytochemical staining of cultured SCG neurons. Staining with anti-KIF3B antibody can be observed throughout the neuron, and is especially evident in axons. When viewed at higher magnification (C), a punctate staining pattern, suggestive of vesicular components, was also noted. B, DIC image of the same cell. D, Western blotting of mouse SCG extract probed with the anti-KIF3B antibody (lane 1). A single distinct band appears at a height corresponding to that of KIF3B, whereas no band is seen with preimmune serum (lane 2). Bars: (A and B) 20 μm; (C) 1 μm. Molecular weight bars in D (from top to bottom): 200, 116, 97, and 65 kD.

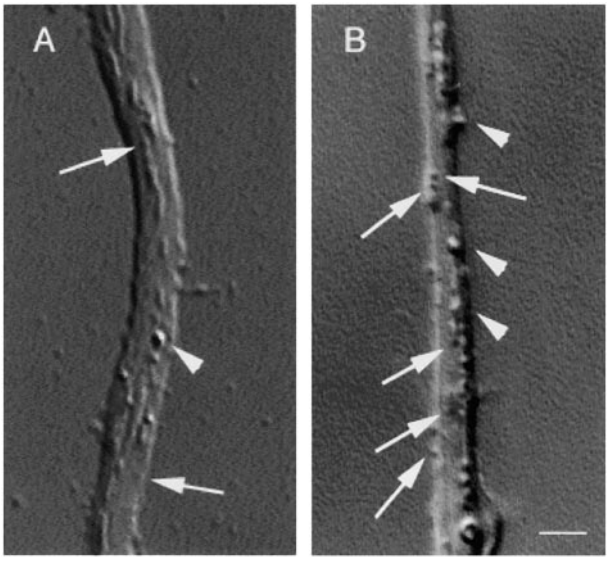

Figure 2. Examples of VEC–DIC images of SCG neuronal axons. SCG neurons grown on collagen type IV-treated coverslips were microinjected with either anti-KIF3B Fab or control normal mouse IgG Fab, and observed under VEC–DIC ~3 h after microinjection. Microinjection of anti-KIF3B Fab brought about a decrease in the number of vesicles within the axons (A), whereas relatively ample vesicle traffic was seen in the axons microinjected with normal mouse IgG Fab (B). The arrowheads depict large vesicles; arrows indicate small vesicles. Bar, 1 μm.

body injection on the mitochondrial motility (data not shown). Thus, we consider that this decreased traffic resulting from anti-KIF3B Fab injection was due to specific effects exerted on only vesicles transported by the KIF3 motor. Considering the resolution limit of the VEC–DIC system, it was almost impossible to discriminate and classify each vesicle by size. Therefore, we could categorize visually observed vesicles into only two groups: large and bright, or small and dark, which might represent endosomal vesicles and small membranous vesicles, respectively, as the former tend to move centripetally.

Neurite Extension Was Inhibited by Anti-KIF3B Fab

Since anti-KIF3 Fab blocked axonal vesicle traffic as described above, *kif3A*$^{-/-}$ and *kif3B*$^{-/-}$ embryos displayed neuronal abnormality (Nonaka et al., 1998; Takeda et al., 1999), and several lines of evidence implied the roles of KIF3 in fast axonal transport (Yamazaki et al., 1995; Ray et al., 1999), we speculated that the KIF3 motor possibly transports the components required for sprouting, construction, and maintenance of axons, which may be blocked by antibody microinjection, resulting in the failure of axonal elongation. To test this hypothesis, we carried out an experiment according to the following scheme.

Instead of microinjecting antibodies into SCG neurons with almost fully extended processes, we now injected cells (n = 60) harboring no neurites, ~12 h after plating. The concentrations of Fab fragment for both anti-KIF3B antibody and normal mouse IgG were adjusted to 3 mg/ml. In the case of control normal mouse IgG Fab (n = 50; Fig. 4, A and B), most of the neurons developed a single axonal structure with branching ~12 h after microinjection. In many cases, axons extended to >100 μm in length, exhibiting active growth cones, and some axons were >300-μm long (Fig. 5). However, microinjection of anti-KIF3B Fab blocked the sprouting of neurites (Fig. 4, C and D), leaving most of the cells without neurites or with miniature sproutings. The median value (Fig. 5) of the axonal sprout length 12 h after microinjection revealed significant differences between the two groups (median values for each

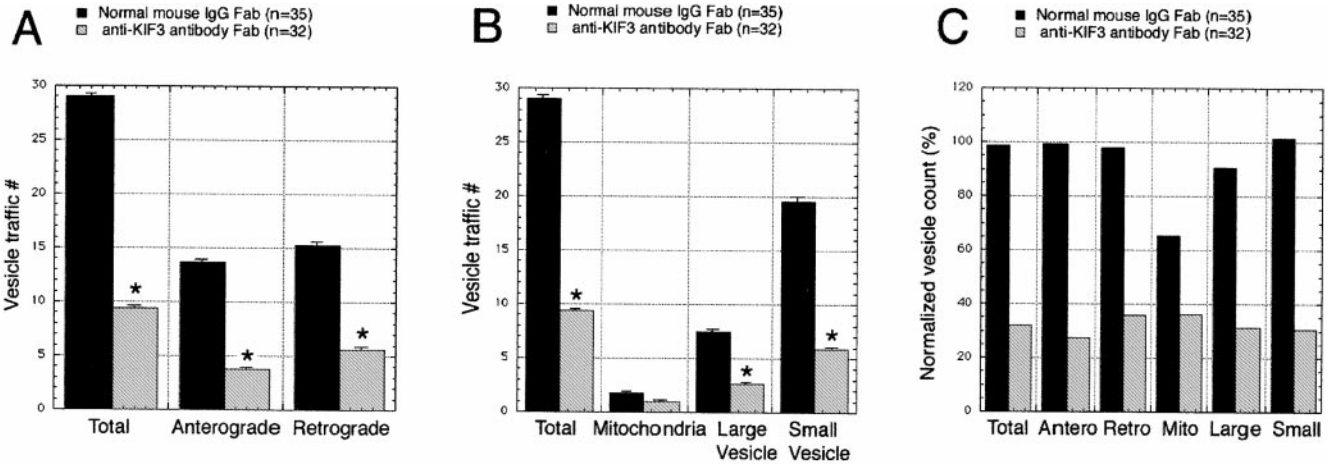

Figure 3. Comparison of vesicle traffic before and after microinjection of Fabs. A, Bidirectional effect of anti-KIF3B Fab microinjection. Both antero- and retrograde traffic were inhibited by the microinjection of the Fab fragments, although the degree of inhibition of the anterograde traffic was stronger. B, Each category of vesicles was counted by the number passing through a unit square (see Observation and Data Collection in Material and Methods, $n/\mu m^2$/5 min) of axonal cross-section. A significant decrease in vesicle traffic was recorded, except in mitochondria. Five comparisons yielded significant P values ($P < 0.05$; *). Bars indicate SEM. C, Normalized vesicle traffic calibrated with that of uninjected cells. For both KIF3B Fab- and normal mouse IgG Fab-injected cells, the number of vesicles passing through a unitary axon transverse section was divided by that in uninjected cells. Note that the injection process, per se, did not have any deleterious effect on the vesicle traffic (the normal mouse IgG Fab group exhibited nearly 100% vesicle traffic in almost all subcategories, compared to the uninjected group).

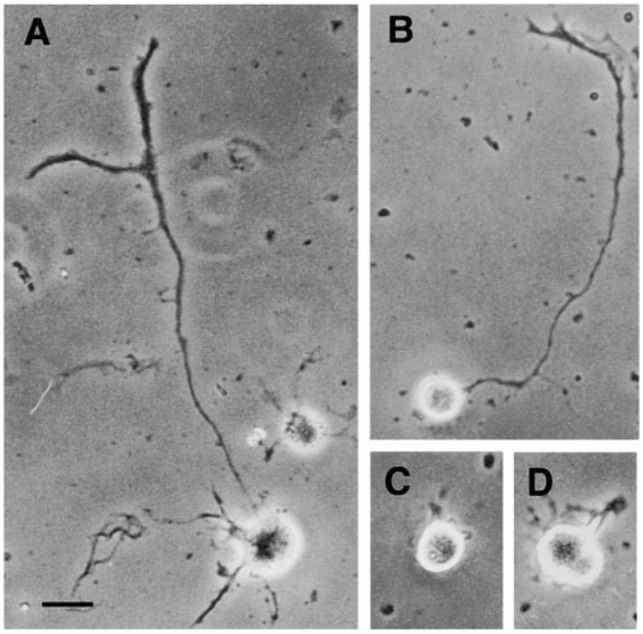

Figure 4. Neurite sprouting was affected by microinjection of anti-KIF3B Fab. Either anti-KIF3B Fab or normal mouse IgG Fab was injected to the cultured SCG neurons before neurite sprouting. Approximately 12 h after injection, the cells were fixed and viewed by conventional fluorescence microscopy to identify the injected cells. Then, phase-contrast images of identified cells were taken. With normal mouse IgG Fab as the negative control, A and B, the treated cells extended axons in an ordinary fashion with ramification. On the contrary, microinjection of anti-KIF3B Fab, C and D, had a drastic effect, and most of the SCG neurons did not extend any neurites at all or exhibited only miniature neurites. Bar, 20 μm.

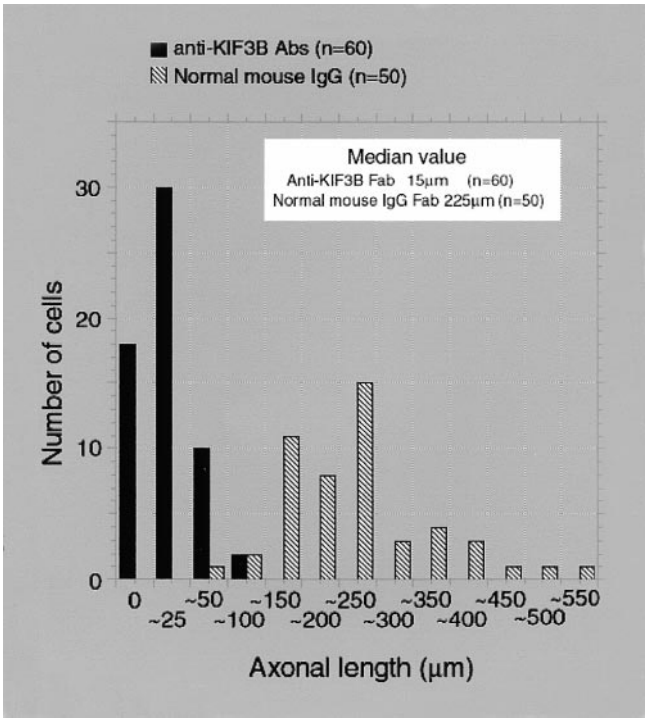

Figure 5. Graphic summary for the axonal length in each experimental group. Distribution of neurite length after microinjection of anti-KIF3B Fab (black) and normal mouse IgG Fab (hatched). Most of the SCG neurons microinjected with anti-KIF3B Fab (n = 60) had short axons, as represented in Fig. 4, C and D, whereas the SCG neurons injected with normal mouse IgG Fab extended their axon normally. The median values for each experimental group show that anti-KIF3B Fab dramatically inhibited (15 μm) axonal outgrowth, compared to normal mouse IgG Fab (225 μm).

group: control, 225 μm; anti-KIF3B Fab, 15 μm), implying the role of the KIF3 motor in neurite sprouting/elongation.

KIF3 Motor Interacts with the Fodrin Molecule

We attempted to further characterize the properties of the vesicles transported by the KIF3 complex. However, the relatively weak and rather transient nature of the binding between the cargos and the motor protein complex (Cole et al., 1998) prevented us from converting real-time dynamic phenomena into morphological evidence. To overcome this problem, we used the yeast two-hybrid screening. Because previous studies (Shimizu et al., 1996; Yamazaki et al., 1996) suggested the role of KAP3 as an associated protein of the KIF3 complex in intercalating the motor domain and the cargos, we used a part of the KAP3 sequence as a bait. Moreover, KAP3 has an *Armadillo*-conserved sequence that is required for the protein–protein interaction (Gindhart and Goldstein, 1996; Shimizu et al., 1996).

To identify the binding partner of KAP3, we generated a fusion construct of the DNA-binding domain and KAP3 coding sequence (aa 209–384). This fusion protein was used in yeast two-hybrid screening of mouse brain cDNA libraries. We selected several $Leu^+/LacZ^+$ colonies from the screening, and we isolated 17 independent positive clones. Out of these clones, three colonies were found to encode fragments of the fodrin gene (Fig. 6). Analysis of the other colonies is under way to determine the in vivo relevance of their affinity for KAP3.

Furthermore, we constructed a series of deletion mutants of the KAP3 construct to determine the minimal binding domain to the fodrin molecule (Fig. 7). The minimal domain required for binding was located within the region where the *Armadillo* repeat is intercepted by a small insert (aa 209–292). In addition, we quantified the binding affinity of each candidate molecule to KAP3 by measuring β-galactosidase activity in liquid cultures of the yeast. The interaction of KAP3 with α-fodrin (αII-spectrin) was the strongest in the three positive clones (234 U for fodrin, 81–85 U for the other two clones, and 3 U for the control vector; U in an arbitrary scale). Therefore, we focused on fodrin in further experiments.

KIF3 Interacts with Fodrin on the Vesicles that Travel Down Axons

To confirm whether the aforementioned results in the yeast two-hybrid assay reflected specific interaction in vivo, we performed the following two sets of experiments.

First, we prepared vesicles from the cauda equina, which is a thick bundle of axons, because they could be prepared without disrupting interactions of motor with vesicles

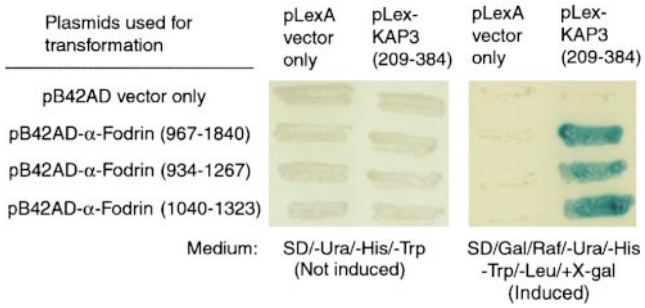

Figure 6. Yeast two-hybrid assay of KAP3 with vesicle-associated proteins. After a yeast two-hybrid system screening, the interaction of α-fodrin with KAP3 was confirmed reproducibly by retransformation. Yeasts containing each combination of pLexA (no insert or KAP3) and pBD42AD constructs (no insert, α-fodrin of various lengths, aa 967–1840, 934–1267, and 1040–1323) grew on the SD/−His/−Trp/−Ura plate containing glucose (left), although those with only α-fodrin survived (right) on the selection plate (SD/−His/−Trp/−Ura/−Leu containing galactose/raffinose/X-gal/BU salts), showing blue colonies.

(Okada et al., 1995b). Moreover, this source and method enables us to isolate axonal vesicles with high purity by detaching them from MTs in the presence of 1 mM ATP. Therefore, we could avoid possible contaminations of plasma membrane fragments. Immunoprecipitation of these vesicles by using anti-KIF3B– or anti-KAP3–coated beads gave a band that was detected with antifodrin antibody in Western blotting (Fig. 8 C, lanes 1 and 3). This association was further confirmed by immunoprecipitation with antifodrin antibody-coated beads, which could pull down both KIF3B and KAP3 (Fig. 8, A and B, lane 5). Furthermore, as the results of the yeast two-hybrid experiment suggested, the binding of the KIF3 motor with fodrin may be direct, since detergent solubilization after immunoprecipitation did not destroy the interaction between the two molecules. In addition, immunoprecipitation by

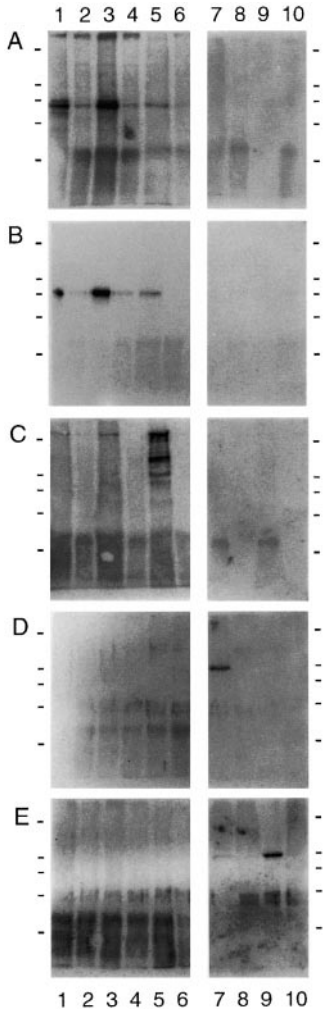

Figure 8. Immunoprecipitation of the vesicle fraction of cauda equina by anti-KIF3B and KAP3 antibodies. Cauda equina vesicles were immunoprecipitated with either anti-KIF3B (lane 1), anti-KAP3 (lane 3), anti–αII-fodrin (lane 5), anti-KIF5A (lane 7), or anti-KIF5B (lane 9) beads. To check the interaction, these immunoprecipitation products were probed with anti-KIF3B (A), anti-KAP3 (B), anti–αII-fodrin (C), anti-KIF5A (D), and anti-KIF5B (E) antibodies. Equal amounts of beads were loaded onto the SDS gel and analyzed by Western blotting under the same condition. Note that the interaction between the KIF3 complex and fodrin could be bilaterally confirmed. Furthermore, fodrin does not associate with KIF5A or KIF5B. In this experiment, immunoprecipitated cauda equina vesicles were solubilized with 1% Triton X-100 for 1 h on ice. The solubilization did not destroy the interaction between fodrin and the KIF3 motor. Lanes 2, 4, 6, 8, and 10 are negative controls immunoprecipitated with the beads treated with the preimmune serum (2, 4, 8, and 10) or normal mouse IgG (6) instead of the specific immunoglobulin for each antigens. Molecular weight bars (from top to bottom): 200, 116, 97, 65, and 45 kD.

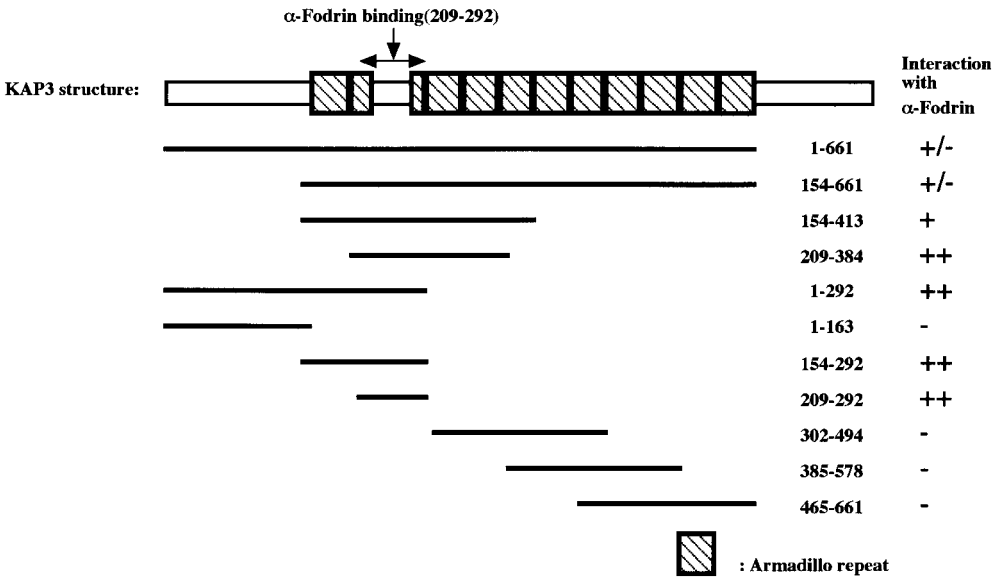

Figure 7. Schematic representation of the functional domain of KAP3 and the α-fodrin molecule obtained by the yeast two-hybrid system. This scheme depicts the entire amino acid sequence of the KAP3 molecule (1–793). We constructed bait vectors of various lengths. The minimal required domain for interaction with fodrin consisted of aa 209–292, as indicated. Determination of the binding affinity using liquid yeast cultures was also performed, and the results are summarized at the right of the figure. The minimal required domain (209–291) showed strongest binding affinity (indicated by ++).

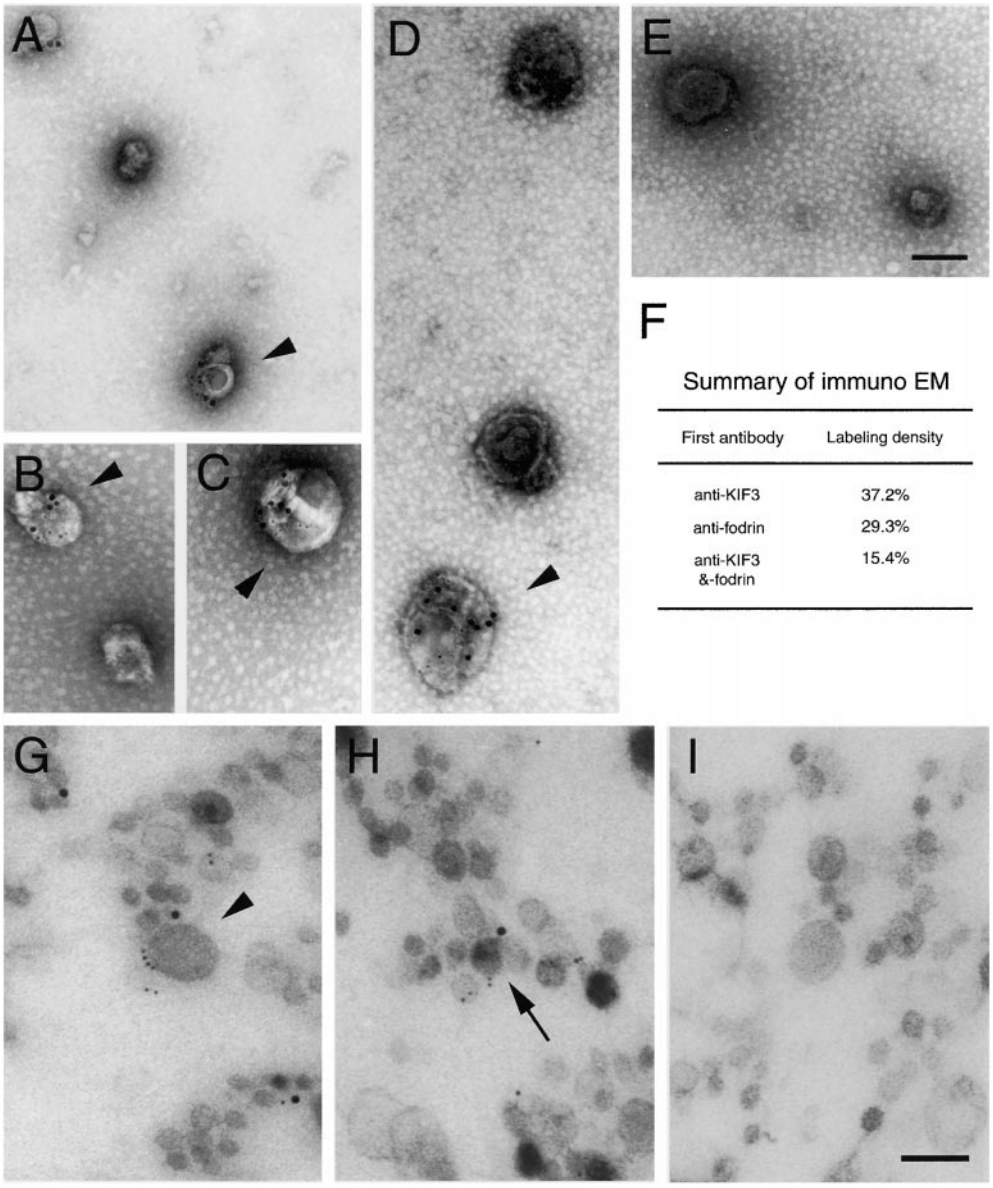

Figure 9. Immuno-colocalization of KIF3 and fodrin on cauda equina vesicles. A–D, Negatively stained cauda equina vesicles containing both KIF3B and fodrin. Vesicles ranging from 50–200 nm in diameter were double-labeled (arrowheads). 10-nm gold particles correspond to the localization of KIF3B and 5-nm gold particles depict αII-fodrin localization. E, Negative control probed with preimmune serum and normal mouse IgG, followed by probing with the auroprobe. No labeling was observed in this panel, but total nonspecific labeling was 4.0%. F, Diagram summarizing the frequency of labeling for KIF3B, fodrin, or both. About 37% of all vesicles contained the KIF3B labeling. G and H, Ultrathin sections of cauda equina vesicles labeled with both anti-KIF3 and αII-fodrin antibody. Compared to the former technique, smaller vesicles, <50 nm in diameter, could be visualized to contain the labeling (H, arrow). I, Negative control incubated with preimmune serum and normal mouse IgG, followed by the reaction with auroprobe. Bars, 100 nm.

using antibodies against other KIFs, such as KIF5A and -B, did not reveal the association of the fodrin molecule to these motor proteins (Fig. 8 C, lanes 7 and 9), suggesting the specific interaction of KIF3 with the fodrin molecule.

Secondly, we carried out two immunoelectron microscopic experiments on the cauda equina vesicles to confirm morphologically the interaction between KIF3 and fodrin. As shown in Fig. 9 F, 15.4% of the vesicles showed both KIF3 (10-nm gold particles) and fodrin (5-nm gold particles) labeling. In the case of single labeling for either KIF3B or fodrin, 37.2 and 29.3% of vesicles were labeled with the two antibodies, respectively. The size of the double-labeled vesicles ranged from 50 to 200 nm in this preparation (Fig. 9, A–D), which partially overlapped with diameters of those immunoprecipitated by anti-KIF3B immunobeads in the previous study (Yamazaki et al., 1995). Colocalization of KIF3B and fodrin was also confirmed in the samples embedded in 2% agarose and epon (Fig. 9, G and H), where relatively smaller vesicles (~30 nm) were found to be double-labeled (Fig. 9 H, arrow).

These data collectively suggest that the interface between the KIF3 motor and cargos might be mediated by fodrin, and those vesicles are transported as fast axonal flow en route to the axonal plasma membrane along MT tracks by KIF3.

Fodrin Travels Down the Axon with the KIF3 Motor

To probe the association of fodrin with the KIF3 motor in vivo, we conducted a radiolabeled pulse–chase experiment in the rat optic nerve. Although the same behavior of fodrin as the KIF3 motor within axons does not necessarily indicate a direct association between the two proteins, and further, with cargos by fodrin to KAP3 binding, it could be strong evidence in this situation, since several batteries of experiments revealed an association between the two proteins.

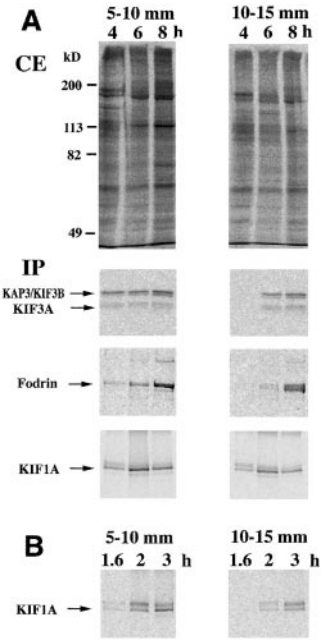

Figure 10. Pulse-labeling study revealing the velocity of KIF3, KIF1A, and fodrin in the rat optic nerve. A, [^{35}S]methionine was injected into the vitreous. 4, 6, and 8 h after administration, the optic nerve and tract were extirpated en bloc and further cut into consecutive 5-mm segments. The second (5–10 mm) and third (10–15 mm) segments were used for the analyses. Note that KIF3 and fodrin bands begin to appear 6 h after treatment. B, Since the reported velocity of KIF1A is much higher than that of KIF3, we killed the animals earlier for determination of the former. In this case, the time of appearance of the KIF1A bands shows good agreement with previous in vitro data, confirming the appropriateness of this system for roughly estimating the velocity of axonal transport. CE, Crude extract; IP, immunoprecipitation.

We injected radiolabeled amino acids ([^{35}S]methionine and [^{35}S]cysteine) into rat eyeballs and chased the newly synthesized proteins by immunoprecipitation. The radiolabeled KIF3 and fodrin moved into the optic nerve and tract toward the lateral geniculate ganglion. Four hours after administration, neither KIF3 nor fodrin was detected in the distal segment (10–15 mm). However, we could identify distinct bands in the proximal segment (5–10 mm); the velocity of fodrin transport was calculated to be between 46 and 51 mm/d (0.5–0.6 μm/sec; Fig. 10 A). Since our previous in vitro motility assay yielded values of 0.53–0.59 μm/s for the KIF3 motor protein (Yamazaki et al., 1996), the obtained value here for α-fodrin velocity shows good agreement with our previous report. The velocity of KIF3 was also in the same range as that of fodrin, whereas KIF1A (12–15 cm/d; 1.4–1.7 μm/sec) was much faster than that of KIF3, confirming the satisfactory resolution and reliability of this method. In this regard, it should be noted that the peaks of moving fodrin and KIF3 are not necessarily the same, even in the case when KIF3 transports vesicles associated with fodrin, because the dynamics of fodrin and KIF3 in the axoplasm, such as their dissociation and association with the vesicles, or their turnover, are possibly different.

Discussion

Anti-KIF3B Fab Blocks Axonal Transport Bidirectionally

We previously reported that KIF3 moves on the MT track to its plus end (Kondo et al., 1994; Yamazaki et al., 1995), which is considered to be an anterograde motor in neuronal axons. However, in the present experiment, microinjection of anti-KIF3 Fab blocked vesicle transport in both directions, although the effect was more marked on the anterograde transport. How can we explain this seemingly ambiguous phenomenon?

First of all, we would like to exclude the possibility of cross-linking of the vesicles into aggregates by the injected antibody, which would be expected to block axonal flow nonspecifically. Retrogradely transported vesicles are especially susceptible to such physical hindrance, due to their large size. To prevent this from occurring, we used monovalent Fab fragments prepared from either anti-KIF3B antibody or normal mouse IgG. Since the Fab fragment has a monovalent property, possible cross-linking by native divalent IgG is avoided. In addition, the more marked inhibition of anterograde transport is also not consistent with this possibility.

Secondly, considering the equilibrium of the membrane pool within axons, it is quite reasonable to speculate that the decreased supply of membranous components to the distal tip of the axon resulted in the reduction of the backflow. Technically speaking, it is also possible that some types of motor proteins responsible for retrograde transport are also attached to the surfaces of vesicles conveyed by the KIF3 complex, so that backflow is also affected in a somewhat indirect manner. Although there are several lines of evidence suggesting that cytoplasmic dynein (CyDy) interacts with fodrin via the dynactin complex (Holleran et al., 1996) and is indispensable for axonal transport (Dillman et al., 1996; Waterman-Storer et al., 1997), we could not directly prove any interaction between KIF3 and CyDy by immunoprecipitation techniques and conventional immunofluorescence microscopy. To date, it is not clear whether the KIF3 motor also conveys a part of the dynein/dynactin complex; some species of anterograde motors probably also carry retrograde motors, such as CyDy, since there is no protein synthesis machinery at the distal end of the axon. Indeed, our previous immunocytochemical study in ligated nerves revealed accumulation of CyDy on both sides of the ligature (Hirokawa et al., 1990). Moreover, recently reported evidence implicates strong dominant genetic interactions among kinesin, CyDy, and dynactin complex mutations in axonal transport in *Drosophila* (Martin et al., 1999). Although it is still premature to presume a similar relationship between KIF3 and CyDy, it might provide a toehold for clarifying the mechanism underlying the bidirectional inhibition.

Finally, it should be noted that as the resolution of VEC–DIC is not sufficient for the complete visualization of all vesicles. The transport of other smaller vesicles or protein complexes that might not be captured by VEC–DIC may also be affected by anti-KIF3 Fab microinjection.

Interrelationship among the KIF3 Motor, Intracellular Transport, and Neurite Sprouting: Implications from our Study

Another remarkable result presented in this study is the inhibition of neurite sprouting and neurite extension by anti-KIF3 Fab injection, the data being consistent with the knowledge that fast axonal transport is required for the advancement of the growth cone (Martenson et al., 1993).

In addition, as Bamburg et al. (1986) reported complete inhibition of axonal growth occurred in the DRG after administration of colcemid, our results also support the assumption that MT-dependent axonal transport is indispensable for the axonal sprouting/elongation process. Taken together, it is reasonable to consider that the KIF3 motor may be involved in axonal sprouting events by supplying materials where they are required. Then, how can we explain the relationship between neurite extension and a cargo of the KIF3 motor? We would like to discuss this material in two directions: vesicular traffic from the Golgi complex to the axonal plasma membrane; and fodrin molecule and neurite sprouting.

As previously reported (Le Bot et al., 1998), the KIF3 motor localizes on the Golgi complex and is responsible for Golgi complex to ER traffic. In our preliminary study, using the Golgi complex preparation from the rat liver (data not shown), KIF3 molecules colocalized with the fodrin molecule on the budding vesicles from the trans-surface of the Golgi complex. Moreover, we immunoprecipitated fodrin with the anti-KIF3 antibody from a vesicle fraction of the cauda equina. The possibility must be considered that KIF3 conveys proteins modified at the Golgi complex and contained in the vesicles pinched off from it to the axonal tips. The colocalization of KIF3B with fodrin on identical vesicles of the cauda equina (Fig. 9, A–D) de facto implies that the situation is analogous with that of CyDy (Holleran et al., 1996). In the case of CyDy, the so-called dynein–dynactin complex binds to the vesicles through the interface between Arp1 and spectrin (fodrin). Although it is not clear whether other components are present in the KIF3 motor, as is the case for CyDy, it could be stated that some vesicles containing fodrin derived from the Golgi complex are transported by the KIF3 motor using the fodrin molecule as a linker protein. Then, they are transported by the KIF3 motor along axonal MTs as a fast component (Cheney et al., 1983), inserted and incorporated into the axonal plasma membrane and cytoskeletal architecture underneath the plasma membrane, because fodrin, together with actin, constitutes the major component of the subaxolemmal cytoskeletal network (Levine and Willard, 1981; Hirokawa, 1982).

From another standpoint, it is plausible that impaired transport of the fodrin molecule, per se, by the KIF3 motor might bring about inhibition of neurite extension. As reported previously, fodrin is concentrated at the growth cone (Sobue and Kanda, 1989), subaxolemmal region (Levine and Willard, 1981), and the abnormally sprouting neurons in Alzheimer's disease (Masliah et al., 1991). In particular, taking the experimental data that fodrin is localized within adhesive sites of growth cone (Sobue and Kanda, 1989) into account, inhibition of axonal elongation could be attributed to the lack of the adhesiveness that generates the traction force for the advancement of the growth cone. Alternatively, miniature sprouting (Fig. 4 C, D) could be a result of subaxolemmal instability, due to the absence of fodrin molecules. For example, α-spectrin mutants of *Drosophila* exhibited pronounced morphological changes in their complex cytoarchitecture, such as in the brush borders of the midgut epithelia (Lee et al., 1993). As the cytoskeletal architecture of the growth cone lamellipodia is similar in certain aspects to that of the brush border, where fodrin and actin constitute the major components of the subplasmalemmal cytoskeletal network (Hirokawa et al., 1983), it is plausible that the phenotype is shared by the two different species and cells. This implies a certain kind of common mechanism controlling motile cellular structure conserved among species.

We would like to express our gratitude cordially to Dr. T. Funakoshi for his help throughout the experiments, Dr. Y. Okada for valuable discussions, and Mr. S. Nonaka for his help with image processing. We appreciate Prof. T. Takenaka and Ms. H. Hashimoto at the Yokohama City University School of Medicine for their instructions on the SCG culture, and the technical advice of Dr. K. Irie at the University of Nagoya on the yeast two-hybrid system. We also thank Dr. M. Kawagishi, Mrs. H. Fukuda, and Ms. H. Sato for their secretarial and technical assistance.

This work was supported by a grant for the Center of Excellence (COE) from the Ministry of Education, Science, Sports and Culture of Japan to Nobutaka Hirokawa. H. Yamazaki and D.-H. Seog were supported by a Japan Society for the Promotion of Science Research Fellowship for Young Scientists.

Submitted: 4 May 1999
Revised: 7 February 2000
Accepted: 9 February 2000

References

Aizawa, H., Y. Sekine, R. Takemura, Z. Zhang, M. Nangaku, and N. Hirokawa. 1992. Kinesin family in murine central nervous system. *J. Cell Biol.* 119: 1287–1296.

Ausubel, F.M., R. Brent, R.E. Kingston, D.D. Moore, J.G. Seidman, J.A. Smith, and K. Struhl. 1997. Current Protocols in Molecular Biology. John Wiley & Sons, Inc. New York. 13.6.2–13.6.5.

Bamburg, J.R., D. Bray, and K. Chapman. 1986. Assembly of microtubules at the tip of growing axons. *Nature.* 321:788–790.

Beech, P.L., K. Pagh-Roehl, Y. Noda, N. Hirokawa, B. Burnside, and J.L. Rosenbaum. 1996. Localization of kinesin superfamily proteins to the connecting cilium of fish photoreceptors. *J. Cell Sci.* 109:889–897.

Brady, S.T. 1985. A novel brain ATPase with properties expected for the fast axonal transport motor. *Nature.* 317:73–75.

Brady, S.T., K.K. Pfister, and G.S. Bloom. 1990. A monoclonal antibody against kinesin inhibits both anterograde and retrograde fast axonal transport in squid axoplasm. *Proc. Natl. Acad. Sci. USA.* 87:1061–1065.

Cheney, R., N. Hirokawa, J. Levine, and M. Willard. 1983. Intracellular movement of fodrin. *Cell Motility.* 3:649–655.

Cole, D.G., S.W. Chinn, K.P. Wedaman, K. Hall, T. Vuong, and J.M. Scholey. 1993. Novel heterotrimeric kinesin-related protein purified from sea urchin eggs. *Nature.* 366:268–270.

Cole, D.G., D.R. Diener, A.L. Himelblau, P.L. Beech, J.C. Fuster, and J.L. Rosenbaum. 1998. Kinesin-II–dependent intraflagellar transport (IFT): IFT particles contain proteins required for ciliary assembly in *Caenorhabditis elegans* sensory neurons. *J. Cell Biol.* 141:993–1008.

De Camilli, P., S.M. Harris, Jr., W.B. Huttner, and P. Greengard. 1983. Synapsin I (protein I), a nerve terminal-specific phosphoprotein. II. Its specific association with synaptic vesicles demonstrated by immunocytochemistry in agarose-embedded synaptosomes. *J. Cell Biol.* 96:1355–1373.

Dillman, J.F., 3rd, L.P. Dabney, S. Karki, B.M. Paschal, E.L. Holzbaur, and K.K. Pfister. 1996. Functional analysis of dynactin and cytoplasmic dynein in slow axonal transport. *J. Neurosci.* 16:6742–6752.

Elluru, R.G., G.S. Bloom, and S.T. Brady. 1995. Fast axonal transport of kinesin in the rat visual system: functionality of kinesin heavy chain isoforms. *Mol. Biol. Cell.* 6:21–40.

Funakoshi, T., S. Takeda, and N. Hirokawa. 1996. Active transport of photoactivated tubulin molecules in growing axons revealed by a new electron microscopic analysis. *J. Cell Biol.* 133:1347–1353.

Gindhart, G.J, Jr., and L.S.B. Goldstein. 1996. *Armadillo* repeats in the SpKAP115 subunit of kinesin-II. *Trends Cell Biol.* 6:415–416.

Higgins, D., P.J. Lein, D.J. Osterhout, and M.I. Johnson. 1991. Tissue culture of mammalian autonomic neurons. *In* Culturing Nerve Cells. G. Banker and K. Goslin, editors. MIT Press, Cambridge, MA. 177–205.

Hirokawa, N. 1982. Cross-linker system between neurofilaments, microtubules, and membranous organelles in frog axons revealed by the quick-freeze, deep-etching method. *J. Cell Biol.* 94:129–142.

Hirokawa, N. 1996. Organelle transport along microtubules: the role of KIFs. *Trends Cell Biol.* 6:135–141.

Hirokawa, N. 1998. Kinesin and dynein superfamily proteins and the mechanism of organelle transport. *Science.* 279:519–526.

Hirokawa, N., R.E. Cheney, and M. Willard. 1983. Location of a protein of the fodrin-spectrin-TW260/240 family in the mouse intestinal brush border. *Cell.*

32:953–965.

Hirokawa, N., R. Sato-Yoshitake, T. Yoshida, and T. Kawashima. 1990. Brain dynein (MAP1C) localizes on both anterogradely and retrogradely transported membranous organelles in vivo. *J. Cell Biol.* 111:1027–1037.

Holleran, E.A., M.K. Tokito, S. Karki, and E.L. Holzbaur. 1996. Centractin (ARP1) associates with spectrin revealing a potential mechanism to link dynactin to intracellular organelles. *J. Cell Biol.* 135:1815–1829.

Kondo, S., R. Sato-Yoshitake, Y. Noda, H. Aizawa, T. Nakata, Y. Matsura, and N. Hirokawa. 1994. KIF3A is a new microtubule-based anterograde motor in the nerve axon. *J. Cell Biol.* 125:1095–1107.

Kozminski, K.G., P.L. Beech, and J.L. Rosenbaum. 1995. The kinesin-like protein FLA10 is involved in motility associated with the flagellar membrane. *J. Cell Biol.* 131:1517–1527.

Le Bot, N., C. Antony, J. White, E. Karsenti, and I. Vernos. 1998. Role of xklp3, a subunit of the *Xenopus* kinesin II heterotrimeric complex, in membrane transport between the endoplasmic reticulum and the Golgi apparatus. *J. Cell Biol.* 143:1559–1573.

Lee, J.K, R.S. Coyne, R.R. Dubreuil, L.S. Goldstein, and D. Branton. 1993. Cell shape and interaction defects in alpha-spectrin mutants of *Drosophila melanogaster*. *J. Cell Biol.* 123:1797–1809.

Levine, J., and M. Willard. 1981. Fodrin: axonally transported polypeptides associated with the internal periphery of many cells. *J. Cell Biol.* 90:631–643.

Marszalek, J.R., P. Ruiz-Lozano, E. Roberts, K.R. Chien, and L.S.B. Goldstein. 1999. Situs inversus and embryonic ciliary morphogenesis defects in mouse mutants lacking the KIF3A subunit of kinesin-II. *Proc. Natl. Acad. Sci. USA*. 96:5043–5048.

Martenson, C., K. Stone, M. Reedy, and M. Sheetz. 1993. Fast axonal transport is required for growth cone advance. *Nature.* 366:66–69.

Martin, M.A, S.J. Iyadurai, A. Gassman, J.G. Gindhart Jr., T.S. Hays, and W.M. Saxton. 1999. Cytoplasmic dynein, the dynactin complex, and kinesin are interdependent and essential for fast axonal transport. *Mol. Biol. Cell.* 10:3717–3728.

Masliah, E., L. Hansen, M. Mallory, T. Albright, and R.D. Terry. 1991. Abnormal brain spectrin immunoreactivity in sprouting neurons in Alzheimer disease. *Neurosci. Lett.* 129:1–5.

Morris, R.L., and J.M. Scholey. 1997. Heterotrimeric kinesin-II is required for the assembly of motile 9+2 ciliary axonemes on sea urchin embryos. *J. Cell Biol.* 138:1009–1022.

Muresan, V., E. Bendala-Tufanisco, B.A. Hollander, and J.C. Besharse. 1997. Evidence for kinesin-related proteins associated with the axoneme of retinal photoreceptors. *Exp. Eye Res.* 64:895–903.

Muresan, V., T. Abramson, A. Lyass, D. Winter, E. Porro, F. Hong, N.L. Chamberlin, and B.J. Schnapp. 1998. KIF3C and KIF3A form a novel neuronal heteromeric kinesin that associates with membrane vesicles. *Mol. Biol. Cell.* 9:637–652.

Nakajima, T., I. Miura, A. Kashiwagi, and M. Nakamura. 1997. Molecular cloning and expression of the KIF3A gene in the frog brain and testis. *Zool. Sci.* 14:917–921.

Nishiye, H., K. Obata, T. Ozaki, and K. Uchizono. 1988. A new method for electron microscopic observation of isolated synaptic vesicles labelled with monoclonal antibody. *Neurosci. Res.* 5:567–576.

Nonaka, S., Y. Tanaka, Y. Okada, S. Takeda, A. Harada, Y. Kanai, M. Kido, and N. Hirokawa. 1998. Randomization of left-right asymmetry due to loss of nodal cilia generating leftward flow of extraembryonic fluid in mice lacking KIF3B motor protein. *Cell.* 95:829–837.

Okabe, S., and N. Hirokawa. 1988. Microtubule dynamics in nerve cells: analysis using microinjection of biotinylated tubulin into PC12 cells. *J. Cell Biol.* 107:651–664.

Okada, Y., R. Sato-Yoshitake, and N. Hirokawa. 1995a. The activation of protein kinase A pathway selectively inhibits anterograde axonal transport of vesicles but not mitochondria transport or retrograde transport in vivo. *J. Neurosci.* 15:3053–3064.

Okada, Y., H. Yamazaki, Y. Sekine-Aizawa, and N. Hirokawa. 1995b. The neuron-specific kinesin superfamily protein KIF1A is a unique monomeric motor for anterograde axonal transport of synaptic vesicle precursors. *Cell.* 81: 769–780.

Pesavento, P.A., R.J. Stewart, and L.S. Goldstein. 1994. Characterization of the KLP68D kinesin-like protein in *Drosophila*: possible roles in axonal transport. *J. Cell Biol.* 127:1041–1048.

Ray, K., S.E. Perez, Z. Yang, J. Xu, B.W. Ritchings, H. Steller, and L.S.B. Goldstein. 1999. Kinesin-II is required for axonal transport of choline acetyltransferase in *Drosophila*. *J. Cell Biol.* 147:507–517.

Rosenbaum, J.L., D.G. Cole, and D.R. Diener. 1999. Intraflagellar transport: the eyes have it. *J. Cell Biol.* 144:385–388.

Shimizu, K., H. Kawabe, S. Minami, T. Honda, K. Takaishi, H. Shirataki, and Y. Takai. 1996. SMAP, an Smg GDS-associated protein having arm repeats and phosphorylated by src tyrosine kinase. *J. Biol. Chem*. 271:27013–27017.

Signor, D., K.P. Wedaman, L.S. Rose, and J.M. Scholey. 1999. Two heteromeric kinesin complexes in chemosensory neurons and sensory cilia of *Caenorhabditis elegans*. *Mol. Biol. Cell.* 10:345–360.

Sobue, K., and K. Kanda. 1989. Alpha-actinins, calspectin (brain spectrin or fodrin), and actin participate in adhesion and movement of growth cones. *Neuron.* 3:311–319.

Takeda, S., T. Funakoshi, S. Okabe, and N. Hirokawa. 1994. Differential dynamics of neurofilament-H protein and neurofilament-L protein in neuron. *J. Cell Biol.* 127:173–185.

Takeda, S., T. Funakoshi, and N. Hirokawa. 1995. Tubulin dynamics in neuronal axons of zebrafish embryos. *Neuron.* 14:1257–1264.

Takeda, S., Y. Yonekawa, Y. Tanaka, Y. Okada, S. Nonaka, and N. Hirokawa. 1999. Left-right asymmetry and kinesin superfamily protein KIF3A: new insights in determination of laterality and mesoderm induction by kif3A$^{-/-}$ mice analysis. *J. Cell Biol.* 145:825–836.

Takenaka, T., T. Kawakami, N. Hikawa, Y. Bandou, and H. Gotoh. 1992. Effect of neurotransmitters on axoplasmic transport: acetylcholine effect on superior cervical ganglion cells. *Brain Res.* 588:212–216.

Tuma, M.C., A. Zill, N. Le Bot, I. Vernos, and V. Gelfand. 1998. Heterotrimeric kinesin II is the microtubule motor protein responsible for pigment dispersion in *Xenopus* melanophores. *J. Cell Biol.* 143:1547–1558.

Vale, R.D., T.S. Reese, and M.P. Sheetz. 1985. Identification of a novel force-generating protein, kinesin, involved in microtubule-based motility. *Cell.* 42: 39–50.

Walther, Z., M. Vashishtha, and J.L. Hall. 1994. The FLA10 gene encodes a novel kinesin-homologous protein. *J. Cell Biol.* 126:175–188.

Waterman-Storer, C.M., S.B. Karki, S.A. Kuznetsov, J.S. Tabb, D.G. Weiss, G.M. Langford, and E.L. Holzbaur. 1997. The interaction between cytoplasmic dynein and dynactin is required for fast axonal transport. *Proc. Natl. Acad. Sci. USA*. 94:12180–12185.

Yamazaki, H., T. Nakata, Y. Okada, and N. Hirokawa. 1995. KIF3A/B: a heterodimeric kinesin superfamily protein that works as a microtubule plus end-directed motor for membrane organelle transport. *J. Cell Biol.* 130: 1387–1399.

Yamazaki, H., T. Nakata, Y. Okada, and N. Hirokawa. 1996. Cloning and characterization of KAP3: a novel kinesin superfamily-associated protein of KIF3A/3B. *Proc. Natl. Acad. Sci. USA*. 93:8443–8448.

Yang, Z., and L.S. Goldstein. 1998. Characterization of the KIF3C neural kinesin-like motor from mouse. *Mol. Biol. Cell.* 9:249–261.